

Chlorine Corrosion Degradation of Low Alloyed Ferritic Steels in Temperature Range 450–550 °C

T. Dudziak¹ · K. Jura² · J. Rutkowska¹

Received: 9 December 2015 / Revised: 12 February 2016 / Published online: 17 March 2016
© The Author(s) 2016. This article is published with open access at Springerlink.com

Abstract The paper shows the results obtained under chlorination conditions on low alloyed steels 15HM (T/P12), 16M (T/P1), 18K, and 10HM2 (T22) in the temperature range 450–550 °C for 100 h. The tests were performed in a gas mixture of 0.3 % Cl₂–Ar under 1 bar pressure. The results indicated that the low alloyed steels underwent a high degree of corrosion, showing lack of protection under reducing atmosphere. However, some differences regarding chemical composition of the bare steels were found. The scale thicknesses, chemical compositions of chloride scales developed on the exposed samples were analysed by means of standard techniques including scanning electron microscope coupled with energy X-ray dispersive spectroscopy.

Keywords Chlorination · Power plant · High temperature · Corrosion

Introduction

Electricity today is something usual for developed civilisations; everyone is using electricity in nowadays. Global energy demands increasing each year, on the other hand, more restricted law in European Union introduces new limits, to protect natural resources and environment.

J. Rutkowska has been employed during the project, however now she is not working in Foundry Research Institute (FRI).

✉ T. Dudziak
tomasz.dudziak@iod.krakow.pl

K. Jura
konrad.jura@edf.pl

¹ Foundry Research Institute, Centre for High Temperature Studies, Zakopiańska 73, 30-418 Kraków, Poland

² EDF Polska S.A – R&D Centre, Ciepłownicza 1, 31-587 Kraków, Poland

As mentioned, climate change is the major challenge to be overcome. Climate change originates mainly from human civilisation due to production of greenhouse gases (GHG) such as CO₂. According to latest International Energy Agency (IEA) energy statistics, energy activities are responsible for 69 % of the anthropogenic GHG, of which 90 % is CO₂ [1]. Worldwide, fossil fuels account for 82 % of the total primary energy supply, solid fossil fuel power stations are a key contributor to this CO₂ emission [2]. There is several way to reduce emission of CO₂ gas and global warming. Possible to implementation solutions include carbon capture and storage (CSS) technology [3, 4], replacement of fossil fuels by fuels more environmentally friendly, such as natural gas [5], commissioning new technologies such as ultra-super critical (USC) [6] or advanced ultra-super critical (AUSC) [7] and finally partly substitute coal by biomass [8, 9].

The changes in coal-fired power plants, in respect to temperature and pressure, can be briefly characterised as follows [10]:

- 1) 70 s of twentieth century: $T = 535\text{ }^{\circ}\text{C}/538\text{ }^{\circ}\text{C}$ /up to 16.7 MPa (up to 167 bar),
- 2) 80 s of twentieth century: $T = 540\text{ }^{\circ}\text{C}/560\text{ }^{\circ}\text{C}$ /up to 25.0 MPa (up to 250 bar),
- 3) 90 s of twentieth century: $T = 560\text{ }^{\circ}\text{C}/580\text{ }^{\circ}\text{C}/27.0\text{ MPa}$ (up to 270 bar),
- 4) Turn of the century twentieth to twenty-first: $T = 600\text{ }^{\circ}\text{C}/620\text{ }^{\circ}\text{C}/29.0\text{ MPa}$ (up to 290 bar) USC,
- 5) Up to 2020 of twenty-first century: $T = 700\text{ }^{\circ}\text{C}/720\text{ }^{\circ}\text{C}/350\text{ MPa}$ (up to 350 bar) A-USC.

The oldest type of coal power units operate with 36 % of efficiency; the newest coal power units (A-USC) are operating under 720 °C and 350 MPa (350 bar) with efficiency 50 % and more contrasting to 45 % in ultra-supercritical (USC) power plants operating at 700 °C. Each 1 % increase in overall efficiency can result in as much as 3 % reduction in CO₂ emissions [11]; therefore, 20 % high efficiency gives 60 % CO₂ reduction.

However, higher efficiency means higher operational temperatures and pressure, which can cause serious problems due to their effects in reducing boiler component lifetime, especially when low alloyed steels are used. This means higher corrosion rate especially under harsh conditions, where aggressive gases are producing due to coal contamination with large amount of Cl or S upon burning or co-firing of biomass in coal-fired power plants.

In many conventional and new designed power plants, biomass is introduced up to 20 % [1]. In this units, the low alloyed ferritic/ferritic-perlitic steels are still used mainly for water wall tubes, other elements when moderate temperatures are met up to 550 °C.

Biomass fuel contains large amounts of Cl. The most severe corrosion problems in biomass-fired energy systems occur due to HCl formation, Cl₂-rich environment and finally Cl₂-rich deposits.

A common hypothesis regarding chlorine-induced high-temperature corrosion is that chlorine in the form of alkali chloride reacts at a steel surface at temperatures higher than 450 °C and actively increases the degradation of the magnetite protective layer. The process is named in some cases as “active oxidation” in which

a “chlorine cycle” is assumed to be involved. This has been visualised by Vaughan et al. [8]. Chloride corrosion is especially dangerous at reducing conditions, which are present during co-combustion of biomass in pulverised boilers.

Because Cl-induced corrosion is still a matter of concern in biomass co fired power units, in this work, chlorine-induced corrosion in 0.3 % Cl_2 –Ar gas mixture on low alloyed ferritic steels 18K, 16M (T/P1), 15HM (T/P12), and 10H2M (T/P22) in the temperature range of 450–500 °C for 100 h was investigated.

The steels tested in this work are the main representatives of the structural materials in the older type power plants constructed in 70–80s of the twentieth century. In comparison to steels with high contents of Cr and Ni, low alloyed ferritic and ferritic-pearlitic steels have low-thermal expansion coefficient and high-thermal conductivity, still the steels are used in modern pulverised power stations where medium temperature up to 550 °C regimes are met.

The post-exposure investigations were initiated by mass change measurements using highly accurate balance Sartorius CPA225D every 25 h. Macro-investigations were performed using digital single-lens reflex camera (DSLR) Canon EOS 70D coupled with macro-single-lens Canon MP-E 65mm f/2,8 Macro. Finally, micro-scale observations were carried out by means of Scanning Electron Microscope (SEM)—Hitachi 3000 table top microscope operated in backscatter electron mode (BSE). Chemical analyses of the exposed surfaces and cross-sectioned samples were conducted by means of energy X-ray dispersive spectrometry (EDX).

Experimental Procedures

The test specimens (samples) with dimensions of $1 \times 1 \text{ cm}^2$ and thickness of 4 mm were cut from unexploited pipe segments. The samples were cut using a precise saw STRUERS ACCUTOM-50 using diamond cut-off wheel. Following the cutting process, the samples were grounded with different SiC papers (200, 600, and 1200) and polished with diamond suspension paste (1 and 3 μm).

The polished samples were accurately measured using micrometre (length of sample, wall thickness, chord length). Based on the calculations, the surface area has been determined in cm^2 . Further step of the sample preparation is involved in ultrasonic cleaning using ultrasonic bath for 15 min at 40 °C. Finally, the samples were weighted using high accuracy 0.01 mg scale in order to measure the initial mass of the individual material. Chemical composition according to Polish Norm: PN-75/H-84024 of the low alloyed steels used in this work is listed below in Table 1.

High Temperature Tests in 0.3 % Cl_2 –Ar Mixture

Figure 1 shows the experimental setup for chlorination of boiler tubing specimens in 0.3 % Cl_2 –Ar mixture for 100 h at 450, 500 and 550 °C. The test samples have been transferred to the hot zone of the furnace, accurately calibrated prior to the high temperatures tests. One test for one temperature lasted 100 h. Mass change of the samples was measured every 25 h using digital balance with accuracy of 0.01 mg.

According to the illustration presented in Fig. 1, 0.3 % Cl_2 –Ar gas mixture under 1 bar pressure was delivered directly to the furnace. For precise flue gas control, the accurate rotameter was used. The gas mixture was constantly controlled via on-line camera setup using gDMSS HD Lite software. The rotameter was placed between the gas cylinder and the furnace indicating 50 N ml/min (N ml/min at 20 °C, 1 bar—standard conditions). The clean, polished accurately weighted samples were placed on the Al_2O_3 (99.5 %) plate and stirred in the hot zone of the wire wound single zone tube furnace (CARBOLITE). The hot zone of the furnace was controlled using 3216 programmable controller from EUROTHERM.

For health and safety reasons, the reaction zone was kept in 316 stainless steel vessel ended from both sides by 316 stainless steel flanges locked by 4 screws. In addition, the stainless steel vessel was lined with Al_2O_3 tube; the tube was ended by silica glassy ends. The whole system was placed in the laboratory where exhaust mixture of gases was firstly cleaned by NaOH solution and further the gas mixture was directed for neutralisation to fume cupboard and then to ventilation system.

Results and Discussion

Kinetic Data

The graphs presented in Fig. 2a–c show kinetic curves of mass change (mg/cm^2) in time (h) for low alloyed boiler steels exposed in chlorination conditions 0.3 % Cl_2 –Ar mixture at high temperatures. The results indicate that chlorination strongly influences behaviour of low alloyed ferritic steels at high temperatures.

All the steels exposed in chlorination conditions showed similar behaviour where instead of mass gain mass loss was observed, the higher temperature of exposure was performed, and higher mass loss was observed during the experiment. Followed by the test for 50 h at the lowest temperature (450 °C), all the steels showed constant and similar mass gain. The highest mass gain was observed after 100 h for steels with the lowest Cr content (18K and 16M). Further exposure of the low alloyed steels at 500 and 550 °C showed decrease in kinetics. The results clearly show that a little addition of Cr to the bulk materials show lack of improvement in terms of corrosion resistance in chlorination conditions.

The observed mass losses of the exposed each individual steel originated mainly from the formation of phases with low stability, the phases based on Fe–Cl structures [2]. At higher temperature, phases evaporation was accelerated from the metal matrix, reaching its maximum at 550 °C. On the other hand, addition of Cr in 2.25 wt% has shown some increased resistance in contrast to the steels with the lowest Cr content. It is suggested that slightly better corrosion resistance was invoked by the formation of more stable Cr–Cl type phase with higher melting point [12].

Table 1 Chemical composition (wt%) of the steels used in high temperature tests in 0.3 %Cl₂–99 % Ar under 1 bar pressure

Grade	Chemical composition (wt%)									
	C	Mn	Si	P max.	S max.	Cr max.	Ni max.	Cu max.	Mo	Other
K18	0.16–0.22	min.0.60	0.10–0.35	0.045	0.045	0.20	0.35	0.25	–	–
16Mo3	0.12–0.20	0.50–0.80	0.15–0.35	0.04	0.04	0.30	0.35	0.25	0.25–0.35	Al. max 0.02
13Cr-Mo4-4	0.11–0.18	0.40–0.70	0.15–0.35	0.04	0.04	0.70–1.00	0.35	0.25	0.40–0.55	Al. max 0.02
10Cr-Mo9-10	0.08–0.15	0.40–0.60	0.15–0.50	0.03	0.03	2.00–2.50	0.30	0.25	0.90–1.10	Al. max 0.02

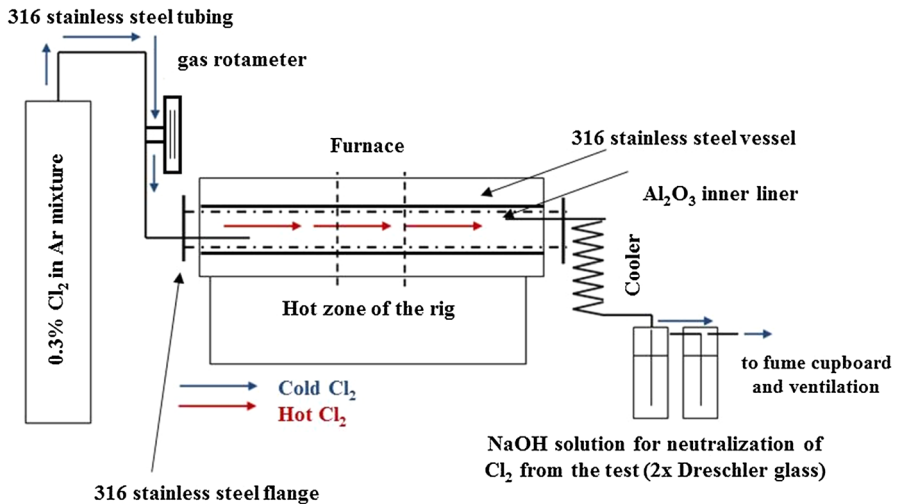


Fig. 1 Schematic illustration of 0.3 % Cl_2 –Ar mixture experimental setup for high-temperature tests at 450, 500 and 550 °C for 100 h

Macro-Observations

The surface analyses after exposures in 0.3 % Cl_2 –Ar mixture test rig were documented using digital camera. The surfaces of the exposed low alloyed steels have shown various rates of degradations; corrosion degradations accelerated with temperature exposure; higher temperature induced higher degradation. Figure 3 shows the surfaces of the exposed materials in the temperature range of 450–550 °C.

The observed surfaces in macro-scale in Fig. 3 show areas of greenish, brownish, yellowish (orange) and finally some violet appearances. Based on the literature and chemical analyses, it can be suggested that the exposed surfaces were covered by $\text{FeCl}_2 \cdot 2\text{H}_2\text{O}$ (green) phase which dehydrates around 140 °C, yellowish (orange) to some extent brownish colour in appearance phase relates to FeCl_3 and $\text{FeCl}_3 \cdot 6\text{H}_2\text{O}$ [13, 14]. Violet appearance of the surface that was observed on the exposed 16M (T/P1), 15HM (T/P12) steels after the tests at 500 and 550 °C was related to anhydrous CrCl_3 phase [15]. Further, the CrCl_3 may react with H_2O to form $\text{CrCl}_3(\text{H}_2\text{O})_x$ phase (where x donates 0.5 or 6) showing dark green appearance of $\text{CrCl}_3 \cdot 6\text{H}_2\text{O}$ phase. The evidence of the formation of low melting compounds based on $\text{FeCl}_3 \cdot 6\text{H}_2\text{O}$ or FeCl_3 (anhydrous) structures in this study is illustrated in Fig. 4. The ends of reaction tube were coated by yellow-orange colour deposit, showing the evidence of the formation of FeCl_3 , $\text{FeCl}_3 \cdot 6\text{H}_2\text{O}$ compound.

Surface Morphologies

Figure 5 shows morphologies after 100 h of exposures in 0.3 % Cl_2 –Ar-mixture used at high temperatures: 450, 500 and 550 °C. The steels with 1 and 2.25 wt% Cr

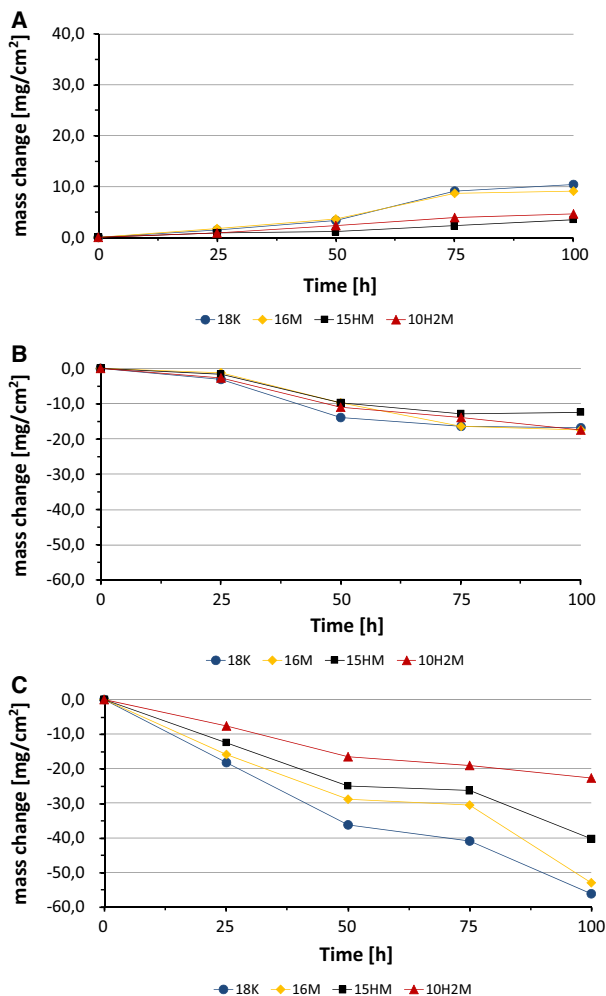
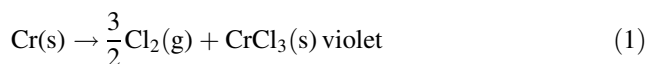


Fig. 2 Kinetic curves for the samples exposed in 0.3 % Cl_2 gas mixture in pure Ar at high temperature **a** 450 °C, **b** 500 °C and **c** 550 °C for 100 h

showed some Cr detection on the surface in the range of 0.5–1 wt%; these findings confirm the formation of violet colour phase representing anhydrous CrCl_3 . Due to the presence of moisture in atmosphere, anhydrous violet CrCl_3 was observed only in some individual places. Reaction with H_2O from the atmosphere led to the transformation of anhydrous CrCl_3 to $\text{CrCl}_3 \cdot 6\text{H}_2\text{O}$, according to the chemical reactions:



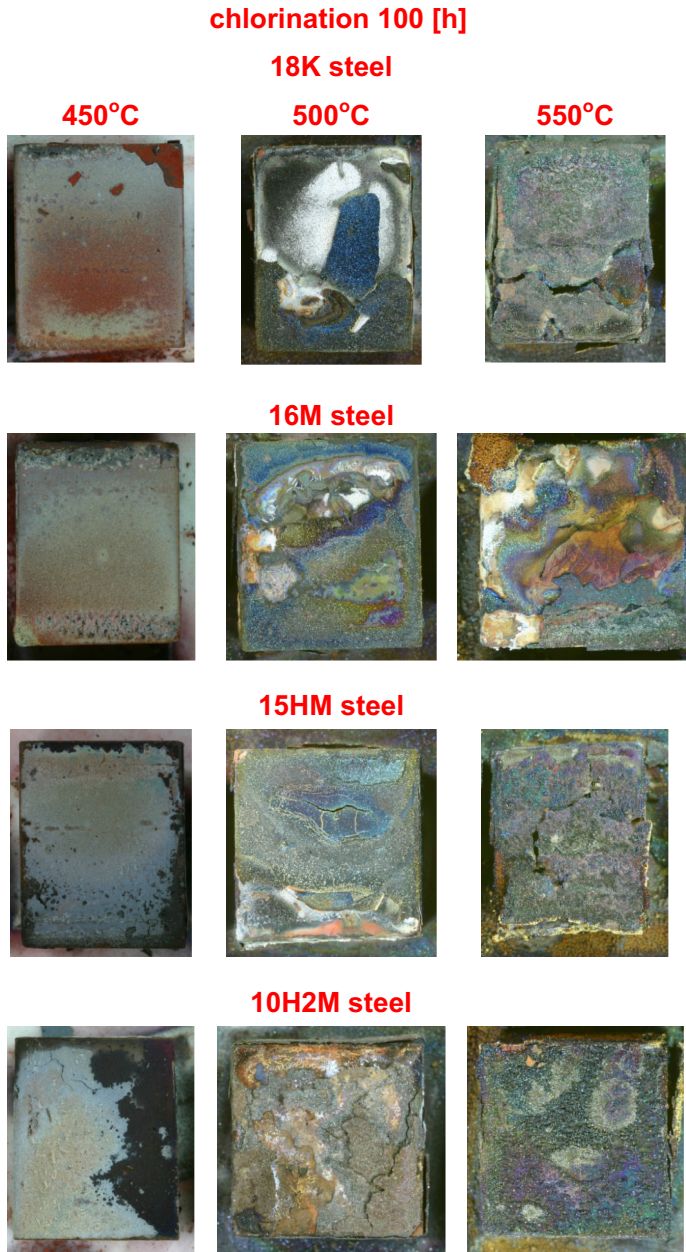


Fig. 3 Macro-images of the exposed low alloyed steels in 0.3 % Cl_2 gas mixture in pure Ar at the high temperatures for 100 h

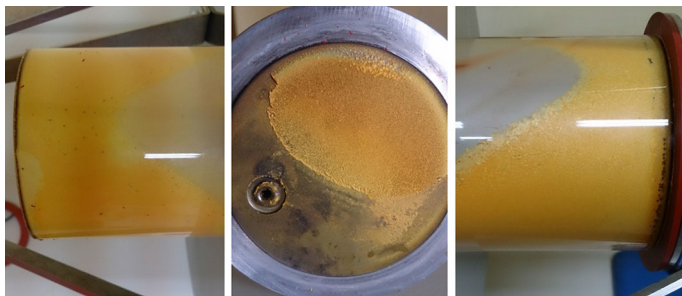
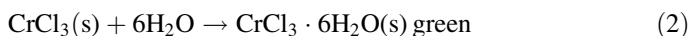
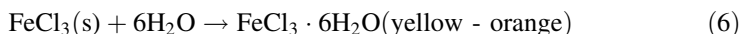
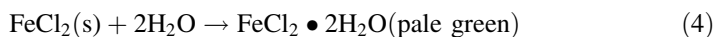
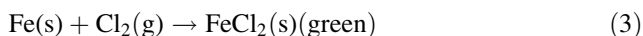


Fig. 4 The $\text{FeCl}_3 \cdot 6\text{H}_2\text{O}$ or FeCl_3 compound deposited on furnace fittings during chlorination in 0.3 % Cl_2 -Ar gas mixture at high temperatures



Similar to CrCl_3 and $\text{CrCl}_3 \cdot 6\text{H}_2\text{O}$, FeCl_2 , FeCl_3 compounds react as well with H_2O leading to the formation of the following phases:



The formation of Cr and Fe chlorides according to study [16] under standard molar Gibbs free energy formation at 25 °C is listed in Table 2.

Based on the values provided in Table 2, it can be suggested that $\text{FeCl}_2 \cdot 2\text{H}_2\text{O}$ and $\text{FeCl}_3 \cdot 6\text{H}_2\text{O}$ should be formed first due to the lowest value of ΔG° [kJ/mol] Gibbs free energy. Hence, consumption of residual oxygen (moist) from the atmosphere provoked the formation of $\text{FeCl}_2 \cdot 2\text{H}_2\text{O}$ and $\text{FeCl}_3 \cdot 6\text{H}_2\text{O}$ and other phases based on Fe–Cl–O structure.

The evidence of chloride(II) formation is the sample 18K exposed at 500 °C for 50 h, which was confirmed by EDX analysis and was shown in Fig. 6. Other sample, exposed beside 18K steel, as well showed the formation of FeCl_2 phase. Figure 7 shows the 15MH (T/P12) steel; similar to 18K at 450 °C it showed development of FeCl_2 phase with composition of 55 wt% Cl_2 and 45 wt% Fe.

To confirm the findings that was presented previously, Fig. 8 shows FeCl_2 – FeCl_3 stability diagram under 1 bar pressure. The diagram represents phases formed upon chlorination conditions using 0.3 % Cl_2 -Ar; the graph was performed using FACTSAGE software with FTSALT database. According to the literature [17] stability diagram, FeCl_3 phase is stable up to 300 °C; further above this temperature, FeCl_3 melted, and therefore volatilisation process occurs. The phase diagram shows that the stability of FeCl_2 is much higher compared to that offered by FeCl_3 . The yellow-orange layer belongs to FeCl_3 compound or if H_2O was presented in the

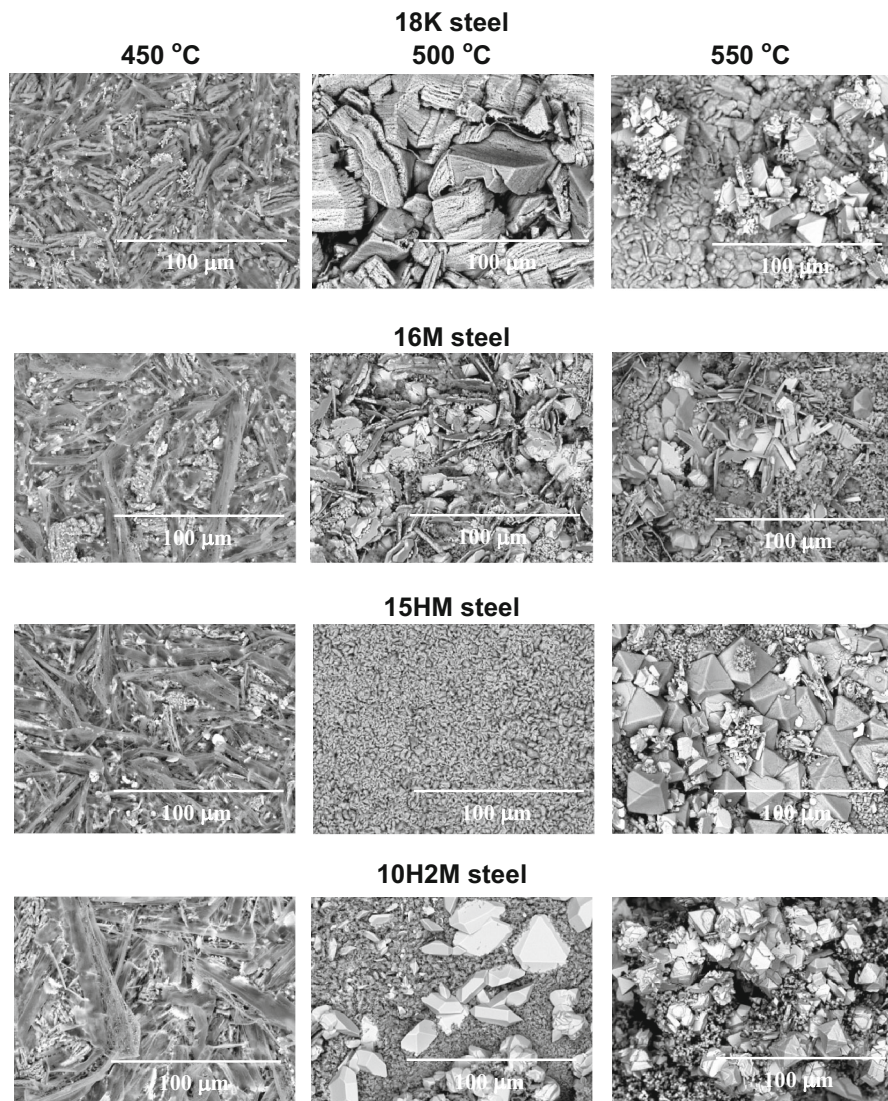


Fig. 5 Surface morphologies of the low alloyed ferritic steels 18K, 16M, 15HM and 10H2M steels, developed after 100 h of chlorination in 0.3 %Cl₂–Ar gas mixture at 450–550 °C

Table 2 Standard ΔG° (kJ/mol) Gibbs free energy formation for chromium and iron chlorides

Compound	ΔG° (kJ/mol)
CrCl ₃	–486.2
FeCl ₃	–334.1
FeCl ₂	–302.3
FeCl ₂ ·2H ₂ O	–797.5
FeCl ₃ ·6H ₂ O	–1812.9

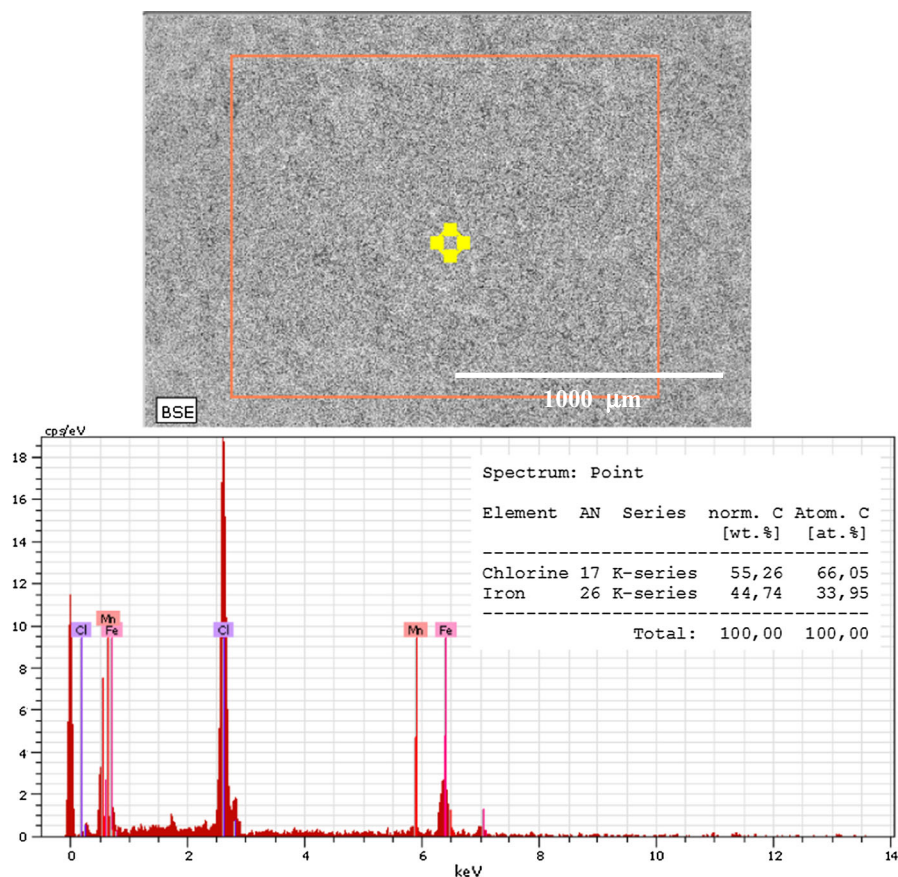


Fig. 6 The EDX analysis of 18K sample after 50 h test in 0.3 % Cl_2 -Ar gas mixture at 500 °C

tested atmosphere $\text{FeCl}_3 \cdot 6\text{H}_2\text{O}$ compounds was likely to form. The process is temperature dependant. At higher temperature, volatilisation accelerates showing higher metal loss. Above melting point of FeCl_3 only FeCl_2 is stable; the phase melts at 677 °C [18].

Cross-Sectional Morphologies

Cross-sectioned images shown in Fig. 9 of the low alloyed ferritic steels exposed to gas mixture 0.3 % Cl_2 -Ar for 100 h at 450, 500 and 550 °C were performed using SEM in BSE mode.

The presented cross-sectioned images show that boiler materials underwent high degree of corrosion degradation indicating poor corrosion resistance against 0.3 % Cl_2 -Ar mixture at 450–550 °C for 100 h. The 18K steel formed porous, fine grain scale with poor adhesion with the metallic substrate. It was found that the steel underwent pitting and intergranular corrosion as well. Chlorine diffusion according

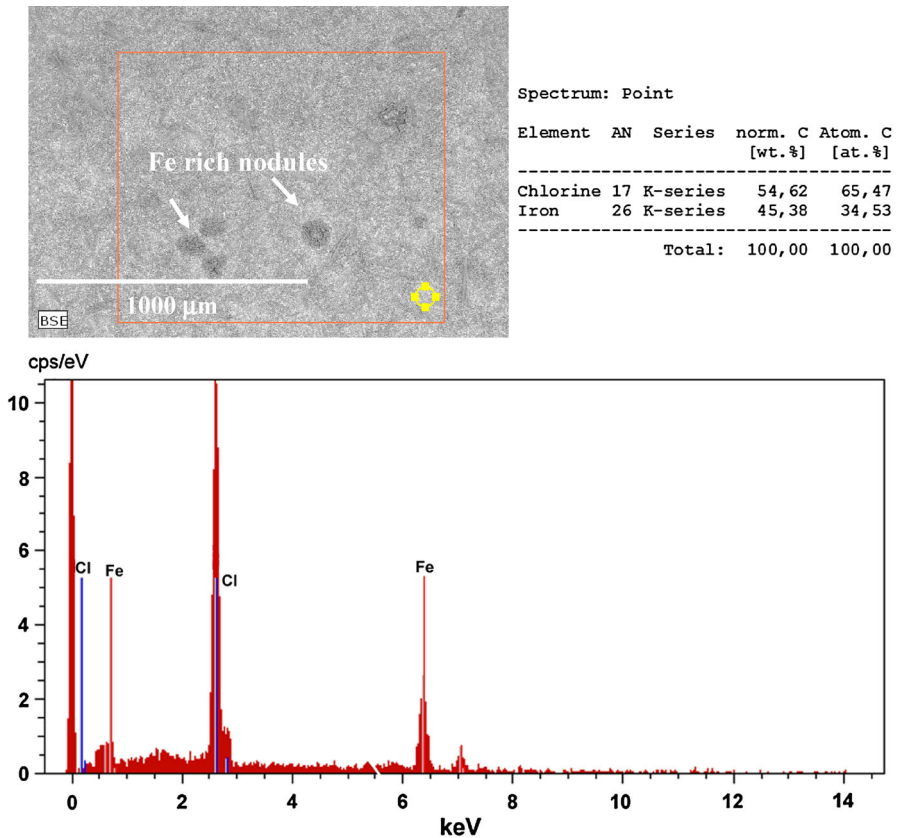


Fig. 7 SEM image in BSE mode of 15MH (T/P12) steel surface and corresponding EDX analysis confirming FeCl_2 phase formation

to the performed calculations reached around 50–60 μm deep inside the material. Similar behaviour and corrosion degradation were found in low alloyed steel 16M (T/P1), whereas chlorine diffused as well for 50–60 μm deep into the material.

Based on the results achieved throughout the EDX analyses, it is assumed that during chlorination of the low alloyed steels phases rich in Fe–Cl structures were formed. The Fe–Cl phases are unstable at high temperatures; during the exposure and dissociation process, free chlorine releases from Fe–Cl phase and diffuses into exposed the material through grain boundaries, pores and other defects. The addition of tiny portion of chromium to ferritic structure shows improvements at high temperatures; however, this improvement is hardly to observe, because the steels with tiny amount of Cr and with slightly higher content of Cr showed similar corrosion resistance.

At the highest temperature (550 °C), high rate of diffusion was found on the surface parallel to the gas stream in 15HM (T/P12) steel (Fig. 10); internal chlorination process was observed under the scale for 150–180 μm throughout grain

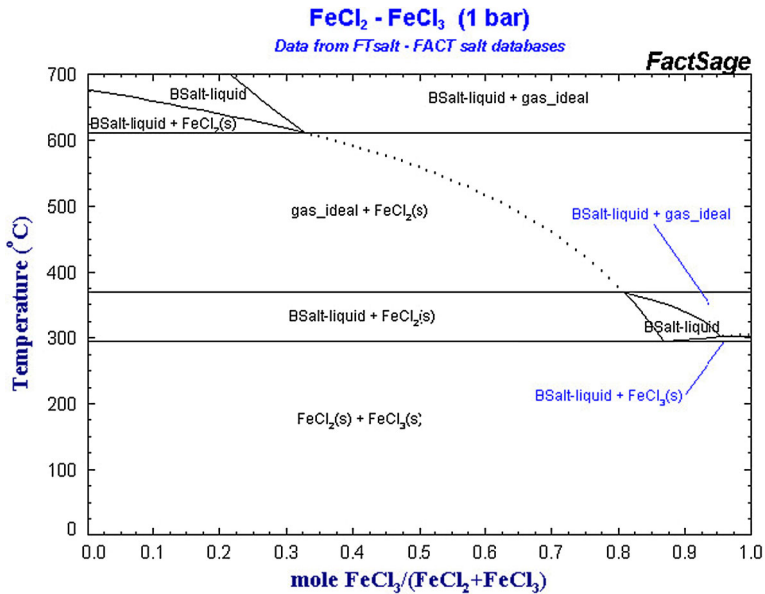


Fig. 8 Stability diagram for FeCl_2 and FeCl_3 compounds at high temperatures

boundaries; however, lack of chlorine inward diffusion was observed on the surface perpendicular to the gas flux.

Assuming that partial pressure of oxygen in 0.3 % Cl_2 –Ar mixture was low, the values are in range of $\log_{10}p(\text{O}_2)/\text{atm} = 10^{-60}$ – 10^{-30} , whereas partial pressure of chlorine was in the range of $\log_{10}p(\text{Cl}_2)/\text{atm} = 10^{-16}$ – 10^{-1} ; it is expected that Cr–Cl and Fe–Cl phases are likely to be formed [19, 20].

Based on the presented phase diagram by Oksa [19], assuming the presence of oxygen (EDX analyses), it is expected that under current test conditions, the formation of iron oxides is likely to occur.

Under oxidising atmosphere, the steels with low Cr content are prone to the formation of non-protective Fe_2O_3 , Fe_3O_4 up to 570 °C; since the tests were prepared in the temperature range 450–550 °C, it is accepted that these two oxides could form.

However, chlorine when concentration is high enough as mentioned previously, it has the ability to diffuse throughout the oxide scale via pores, cracks, and other defects in the iron oxide structure. Such scenario was observed in 15HM (T/P12) steel at 550 °C. At the scale–substrate interface, oxygen partial pressure was low (consumed for the oxide scale formation), thus within the oxide scale FeCl_2 , FeCl_3 and CrCl_3 (in 15HM and 10H2M steels) were developed. When chlorides were developed, oxygen partial pressure increased, again chlorides decomposed, and the formation of metal oxide was observed; however, again formed oxide scale from gas-phase reaction developed a very loose layer with lack of protection to the metal substrate.

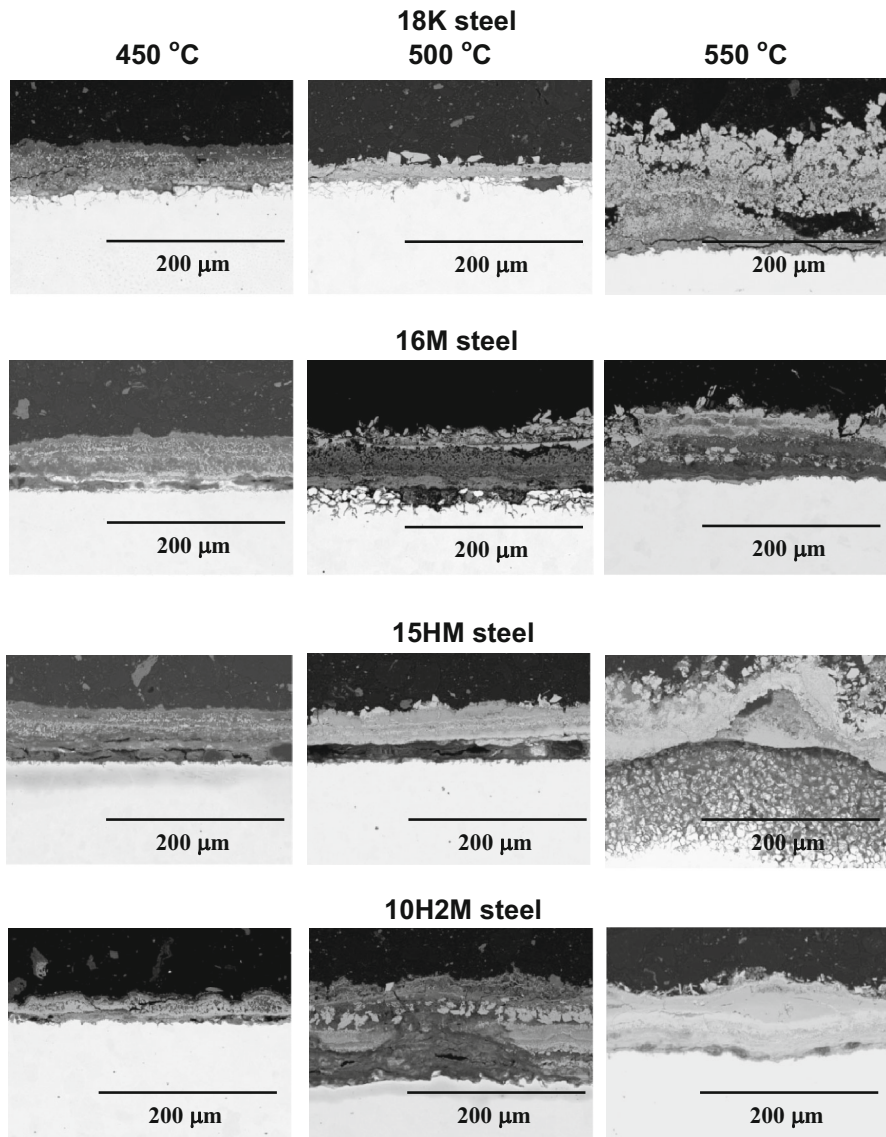


Fig. 9 Cross-sectional images of the low alloyed ferritic steels: 18K, 16M, 15HM and 10H2M exposed in 0.3 %Cl₂-Ar mixture at 450–550 °C for 100 h

Poor corrosion resistance significantly accelerates, because metal chlorides have high vapour pressures even at low temperatures, which can lead to vaporisation and rapid loss of metal from the surface [21], as observed in the current study. The metal chloride is stable and is in solid state only in narrow temperature range, as shown in Fig. 8 and studies presented by Oksa [19] and Grabke [20].

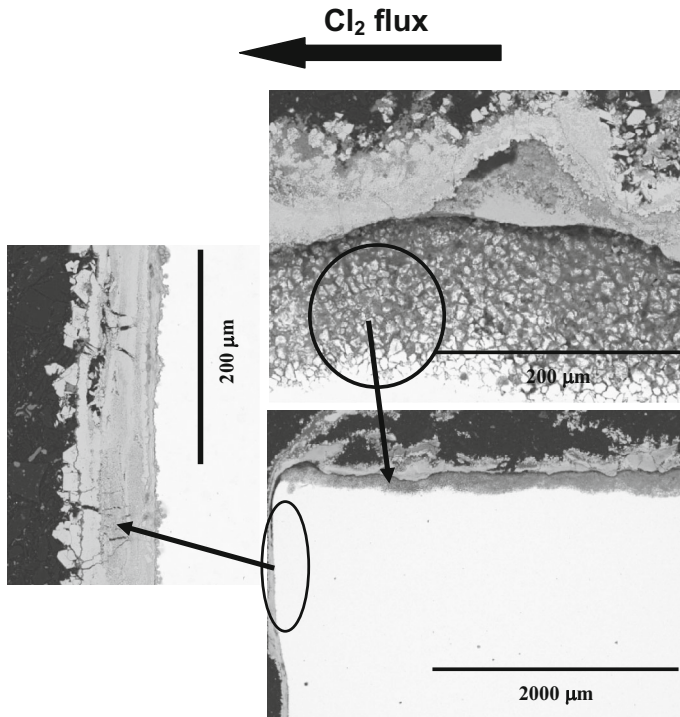


Fig. 10 Corrosion invoked in chlorine gas in 15HM steel under 0.3 %Cl₂–Ar gas mixture at 550 °C

The black circle in Fig. 10 shows the difference of chlorine activity during high-temperature chlorination in 0.3 %Cl₂–Ar gas mixture at 550 °C. As observed, the sides of the sample showed the formation of the scale adherent to the surface of metallic substrate. The surface exposed parallel to chlorine-rich atmosphere showed inward diffusion of chlorine deep inside the metal matrix reaching 150–180 μm; the internal chlorination process was found only in 15HM (T/P12) steel at 550 °C.

Therefore, the 15HM (T/P12) steel underwent high degree of corrosion degradation due to two processes that occurred simultaneously; chlorine produces the formation on the parallel surface to gas flux and secondly internal chlorination process via grain boundaries in the steel matrix. It is assumed that internal chlorination process occurred due to the higher activity of Cl in the gas flux, with the parallel surface than perpendicular direction. Furthermore, the scale showed much lower adhesion to the substrate due to formation of the oxide scale via gas-phase reaction. Low adherence to the metal surface allowed larger amounts of Cl gas to diffuse inwardly, due to much shorter diffusion path than that on the surface perpendicular to the gas flux. Because all the steels exposed in chlorine-rich atmosphere showed high degree of corrosion degradation, the presented corrosion mechanism can be assumed for all the steels exposed in this study. In contrast to Chang et al. [17] results, the test performed at 450 °C in this study indicates that some protective scale formation was found only when Cr addition was given to

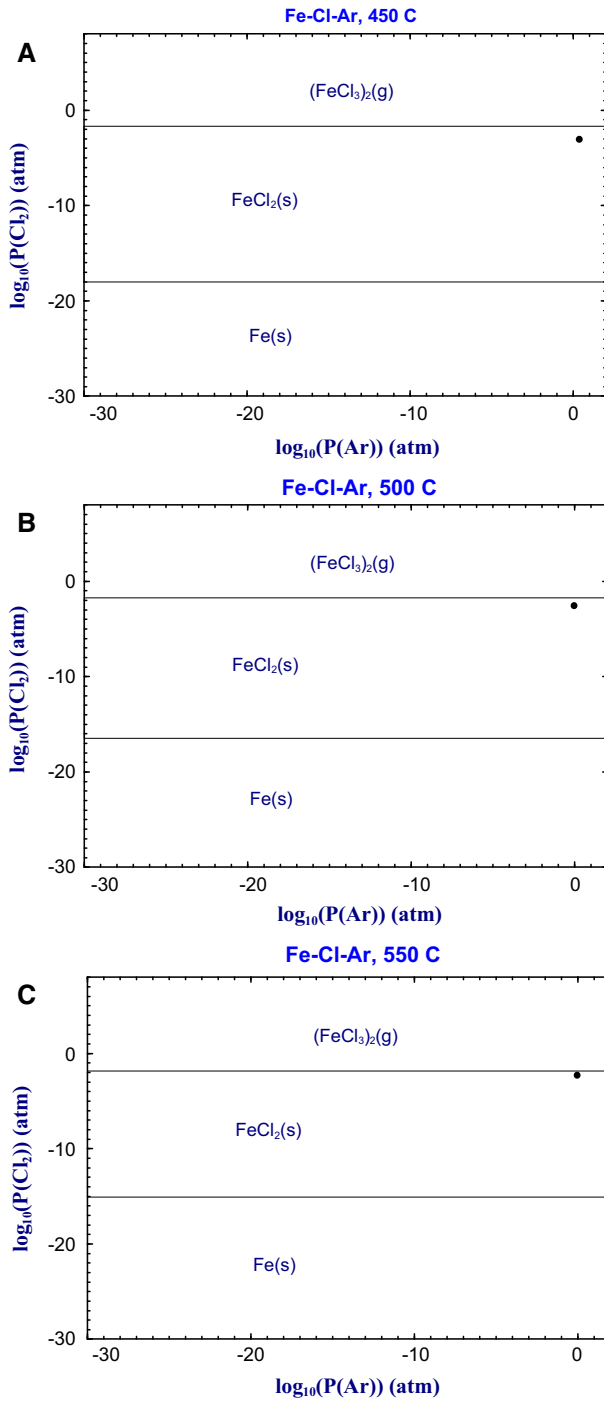


Fig. 11 Stability diagrams for Fe–Cl–Ar system at **a** 450, **b** 500 and **c** 550 °C

15MH and 10H2M steels; in other cases when steel showing lack of Cr addition even at temperatures lower than 500 °C, development of non-protective scale took place.

The results showed in Fig. 11a–c present calculated partial pressure of Cl in experimental 0.3 %Cl–Ar gas mixture for the formation of FeCl_2 and FeCl_3 using FACTSAGE software FTSALT database. Current test conditions on the figures are pointed by black spot. The performed calculations confirm the findings from macro- and micro-observations. The formation of FeCl_2 phase is most probably to occur; EDX results presented in Figs. 6 and 7 showed such evidence. The formation of FeCl_3 is highly probable to develop, since point indicating stability of $\text{FeCl}_3(\text{g})$ phase is above the stability line; however, this phase is unstable above 300 °C and transforms into gaseous state; therefore, EDX analyses performed on the exposed samples found difficulties with the detection of FeCl_3 . As mentioned in this work, the presence of H_2O from the atmosphere leads to the formation of $\text{FeCl}_3 \cdot 6\text{H}_2\text{O}$ compound.

Conclusions

This paper reported the results of a study which was carried out to investigate the effects of 0.3 %Cl₂ in pure Ar under 1 bar pressure environment on corrosion resistance of low alloyed ferritic steels 18K, 16M, 15HM (T/P12) and 10H2M at three temperatures: 450, 500 and finally 550 °C. Based on the findings in the research performed, the following conclusions can be made:

- the low alloyed steels showed poor corrosion resistance in the temperature range of 450–550 °C,
- the exposed steels showed the formation of thick, porous scale consisting different compounds based of Fe–Cl structures,
- addition of 2.00–2.5 wt% Cr showed little effect in chloride-rich atmosphere,
- the formation of volatile phases increasing with increased temperatures producing high rate of mass loss,
- the formation of FeCl_2 phase was confirmed by EDX analyses,
- evaporation of FeCl_3 , $\text{FeCl}_3 \cdot 6\text{H}_2\text{O}$ was found throughout the deposition of yellow-orange coating in glassy part of the high-temperature rig,
- the 15HM (T/P12) steel showed formation of corrosion products on the exposed surfaces and inner chlorination process throughout grain boundaries.

Acknowledgments The authors would like to acknowledge the financial support of EDF Poland. The study was a part of the project “Fundamental research of high temperature resistance of boiler steels—EDF Poland”. Grant Number: R&D/ZN/KWA/04072014/099.

Open Access This article is distributed under the terms of the Creative Commons Attribution 4.0 International License (<http://creativecommons.org/licenses/by/4.0/>), which permits unrestricted use, distribution, and reproduction in any medium, provided you give appropriate credit to the original author(s) and the source, provide a link to the Creative Commons license, and indicate if changes were made.

References

1. C. Henderson, in *Co-firing of Biomass in Coal-Fired Power Plants—European Experience*, IEA Clean Coal Centre, *Presentation at FCO/IEA CCC Workshops on Policy and Investment Frameworks to Introduce CCT in Hebei and Shandong Provinces* (2015).
2. B. R. Tarr, H. S. Booth and A. Dolance, *Inorganic Syntheses* **3**, 191 (1950).
3. R. Wennersten, Q. Sun and H. Li, *Journal of Cleaner Production* **103**, 724 (2015).
4. R. M. Cuéllar-Franca and A. Azapagic, *Journal of CO₂ Utilization* **9**, 82 (2015).
5. S. Ševik, *Renewable and Sustainable Energy Reviews* **52**, 572 (2015).
6. S. Hasti, A. Aroonwilas and A. Veawab, *Energy Procedia* **37**, 2544 (2013).
7. P. S. Weitzel, J. M. Tanzosh, B. Boring, N. Okita, T. Takahashi, and N. Ishikawa, in *Advanced Ultra-supercritical Power Plant (700 to 760°C) Design for Indian Coal*, *Power-Gen Asia Conference* (2012).
8. D. A. Vaughan, H. H. Krause, and W. D. Boyd, in *Proceedings of the International Conference on Ash Deposits and Corrosion from Impurities in Combustion Gases* (1977).
9. H. J. Grabke, E. Reese and M. Spiegel, *Corrosion Science* **37**, 1023 (1995).
10. T. U. Kern, K. Weighardt, and H. Kirchner, in *Material and Design Solutions for Advanced Steam Power Plants Proceedings of the 4th International Conference on Advances in Materials Technology for Fossil Power Plants* (2004).
11. J. Henry, G. Zhou and T. Ward, *Materials at High Temperatures* **24**, 249 (2007).
12. A. F. Wells, *Structural Inorganic Chemistry*, 5th ed, (Oxford University Press, Oxford, 1984).
13. A. F. Trotman-Dickenson (ed.), *Comprehensive Inorganic Chemistry*, (Pergamon, Oxford, 1973).
14. A. F. Holleman and E. Wiberg, *Inorganic Chemistry*, (Academic Press, San Diego, 2001).
15. B. Mills, *Sample from Aldrich (99%, Sublimed), CAS # 10025-73-7, Photograph of a Sample of Anhydrous Chromium(III) Chloride, CrCl₃* (2009).
16. http://www2.ucdsb.on.ca/tiss/stretton/database/inorganic_thermo.htm.
17. Y. N. Chang and F. I. Wei, *Journal of Materials Science* **26**, 3693 (1991).
18. N. S. Gill and F. B. Taylor, *Inorganic Synthesis* **9**, 136 (1967).
19. M. Oksa, in *Nickel- and Iron-Based HVOF Thermal Spray Coatings for High Temperature Corrosion Protection in Biomass-Fired Power Plant Boilers*, VTT, *Technical Research Centre of Finland Ltd* (2015).
20. H. J. Grabke, in *Incinerating Municipal and Industrial Waste*, ed. R. W. Bryers (Hemisphere, New York, 1989).
21. H. P. Nielsen, F. J. Frandsen, K. Dam-Johansen and L. L. Baxter, *Progress in Energy and Combustion Science* **26**, 283 (2000).